JOURNAL OF CHEMICAL & ENGINEERING DATA

ARTICLE

pubs.acs.org/jced

Complex Formation, Metal Uptake, and Sorption Kinetics of a Chemically Modified Chlorosulfonated Polystyrene with Aminosalicylic Acid

Ali El-Dissouky,* Abdel-Zaher Elassar, and Abdul-Hadi Bu-Olian

Chemistry Department, Faculty of Science, Kuwait University, P.O. Box 5969, Safat 13060, Kuwait

ABSTRACT: The resin ($PsSO_2ASA$) was synthesized by the reaction of chlorosulfonated polystyrene ($Ps\text{-}SO_2Cl$) with 4-aminosalicylic acid (ASA) and characterized by elemental analysis, SEM, EDS, and FT-IR spectral studies and thermal analysis. Its metallopolymer complexes with Co(II), Ni(II), and Cu(II) ions were examined with respect to various experimental parameters. The spectral (FT-IR, electronic, and ESR) studies confirmed that the octahedral complexes formed and the resin bonded to the metal ion through the carboxylato- and phenolato-O atoms. The metal sorption by the resin from aqueous solutions at different conditions was investigated by batch and column methods utilizing ICP−AES. Kinetic studies showed that the adsorption of metal ions onto the resin proceeds according to the pseudosecond order model, and the equilibrium data was best interpreted by the Langmuir isotherm. The sorption capacity was observed in the order of Cu(II) > Co(II) > Ni(II). The calculated thermodynamic parameters indicated an endothermic spontaneous sorption accompanied by deprotonation of the resin and liberation of water of hydration of the metal ions and that adsorbed by the free resin. The degrees of freedom increased at the solid−liquid interface during the sorption of the metal ions onto the resin. The lower detected concentration by the method was found to be (10 to 20) ng mL^{-1}. The method was successfully applied to the analysis of natural water samples.

1. INTRODUCTION

Contamination by heavy metals is recognized as a priority issue in environmental protection. Metal ions such as copper, lead, mercury, cadmium, cobalt, iron, and so on represent an environmental concern when present in uncontrolled or high concentrations. For example, elevated copper concentrations are frequently associated with leaching from antifouling paints and pressure-treated dick pilings, discharge from power and desalination plants and runoff from land-based sources.[1−5] Also copper, nickel, cobalt, lead, iron, and other heavy elements are present in the acidic manganese chloride solution resulting from the preparation of battery grade MnO_2 directly from manganese ore.[6−8] Due to their persistence in the environment and their relatively rapid uptake and accumulation in living organisms, heavy metal ions are polluting water sources and posing a long-term risk to both humans and the eco-system. Therefore, the determination of trace concentrations of metal ions in man made and natural water sources is essential in order to keep a check on the various eco-systems. Hence, this requires frequent analysis of trace metal ions in environmental as well as biofluid samples in order to sustain and preserve the eco-systems.

The determination process is not simple because the metal ions are surrounded and encapsulated by a variety of complex matrix species.[9] The direct determination of metal ions in effluents or in saline matrices (e.g., seawater) by atomic spectrophotometry as flame or plasma techniques is difficult due the high background, transport, and chemical interferences which result in a decrease in precision and sensitivity. Therefore, separation and preconcentration methods have played a fundamental role in solving these problems. Accordingly, there is a need for an extraction technique which could selectively extract the analytes of interest. This has paved the way for the development of solid phase extraction (SPE) techniques. The SPE provides several major advantages over the classical liquid extraction technique: (i) fast, simple and direct sample application in very small quantities (microliter volume) without any sample loss, (ii) no waste generation as derived in liquid extraction technique, (iii) SPE can be interfaced with major chromatographic techniques either in online or off-line mode, and (iv) time and cost efficiency.[9−11]

Chelating polymeric matrices, termed polychelatogens (PC),[10] have been used in the SPE technique. It has several highlighting features such as a high degree of selectivity, versatility, durability, and good metal loading capacity and enhanced hydrophilicity.[11,12] The donor atoms involved in forming chelates usually include oxygen, nitrogen, phosphorus, and sulfur atoms present in phenol, carbonyl, carboxylic, hydroxyl, ether, phosporyl, amine, nitro, nitroso, azo, hydrazo, diazo, nitrile, amide, thiol, thioether, thiocarbamate, and bisulphite compounds.[10] The selectivity of the surface with the immobilized functional groups toward metal ions depend on the size of the modifier,[9] the activity of the loaded group[13] and the characteristics of the hard−soft acid−base.[13,14]

Several chelating supports have been used in the past[15−31] of which the use of polystyrene-divinylbenzene (Ps-DVB) resin has been found to be fruitful. These can be easily functionalized as well as loaded with a variety of organic ligands with different functional groups.[11,21−31] The Ps-DVB resin beads are commercially available as the Amberlite XAD series, which differ in their degree of cross-linking, bead size, pore diameter, etc. which

Received: August 4, 2010
Accepted: March 11, 2011
Published: March 23, 2011

directly influence the rate and the degree of metal sorption. Several papers on Amberlite XAD and its chloromethylated derivatives have referred to the preparation of different chelating resins for studying their metal uptake capacity, selectivity, and preconcentration.[15−31] Moreover, it is found that the use of a hydrophilic chlorosulfonyl group as the anchoring linkage for the synthesis of various supported ligands gives significant advantage over the more widely used chloromethyl group with emphasis on high capacity and decreased toxicity in the selective studies of predisposed, polymer pendant ligands.[13−32]

As a part of our continuing effort to design new and effective chelating resins of high metal uptake and selectivity, we aim to (i) synthesize and characterize the chemically modified chlorosulfonated polystyrene with aminosalicylic acid chelating resin ($PsSO_2ASA$) and its Cu(II), Ni(II), and Co(II) complexes; (ii) determine the factors affecting the Cu(II), Ni(II), and Co(II) sorption from aqueous solutions and study the sorption kinetics and equilibria by the batch and column methods; (iii) apply the recommended method for the analysis of Kuwaiti tap water and Arabian Gulf water. Inductively coupled plasma atomic emission spectrometry (ICP−AES) has been used to determine the metal uptake and the concentration of Cu(II), Ni(II), and Co(II).

Scheme 1. $PsSO_2ASA$

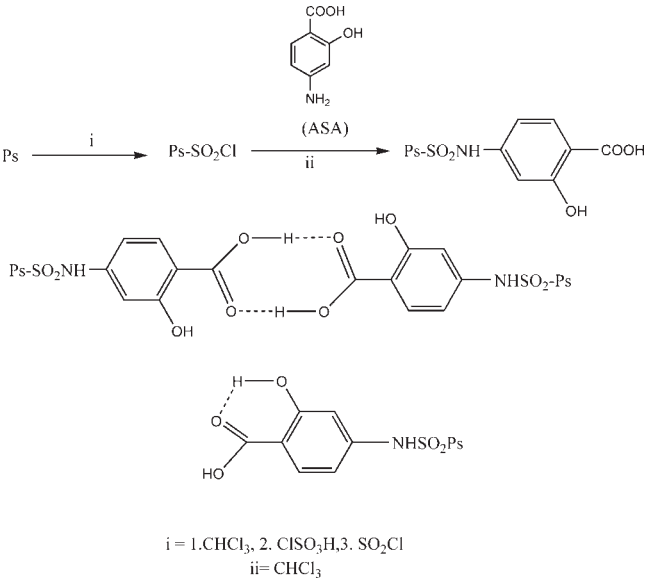

i = 1.$CHCl_3$, 2. $ClSO_3H$,3. SO_2Cl
ii= $CHCl_3$

2. EXPERIMENTAL SECTION

2.1. Reagents and Solutions. All chemicals used in this work were of analytical grade from Merck (Germany). Commercially, available Amberlite XAD-16 (specific area 800 $m^2\ g^{-1}$ and bead size (3.4 to 10.2) mm was obtained from Aldrich and it was thoroughly washed with 4.0 mol L^{-1} HNO_3, 1.0 mol L^{-1} NaOH, and double distilled water successively and well dried before use. 4-aminosalicylic acid and chlorosulfonic acid were purchased from Aldrich and used as received. $Cu(NO_3)_2\cdot 2.5H_2O$, $Ni(NO_3)_2\cdot 6H_2O$, and $Co(NO_3)_2\cdot 6H_2O$ were purchased from Aldrich and used without further purification. Working metal ion solutions (0.1 mol L^{-1}) of Cu(II), Ni(II), and Co(II) were prepared by dissolving $Cu(NO_3)_2\cdot 2.5H_2O$, $Ni(NO_3)_2\cdot 6H_2O$, and $Co(NO_3)_2\cdot 6H_2O$ in acidified double distilled water. The glassware used were soaked in 10% HNO_3 overnight before use and cleaned repeatedly with double distilled water.

2.2. Elemental Analysis and Instrumentation. CHN analysis was performed on a LECO CHNS-932 elemental analyzer. The concentration of the metal ions was determined by ICP−AES. The wavelengths used for the analysis of Cu(II), Ni(II), and Co(II) were (324, 231, and 238) nm, respectively. A digital Orion pH/ISE meter- model 710 A, was used for the pH measurements. The pH values of the solutions were adjusted with monochloroacetic acid/acetate buffer in the pH range 2.5 to 4.0, acetate buffer in the pH range 4 to 7. Hydrochloric acid was used to adjust the pH below 2.5. Fourier Transform Infrared (FT-IR) spectra of the chelating resins and their complexes as KBr discs were recorded with a Schimadzu 2000 FT-IR spectrophotometer. Electronic spectra of the chelating resin and its complexes were recorded with a Varian Cary 5 UV/vis/NIR spectrophotometer. Thermal analyses were carried out on a Shimadzu Thermal system 50 consisting of TGA-50 and DTA-50 in the temperature range of ambient temperature up to 1000 °C under dinitrogen atmosphere with a heating rate of 10 °C/min. For the batch method, the samples were shaken utilizing the Innova™ 3100 digital water bath shaker thermostatted at (250 to 450) rpm. The surface area of the polymer support and its metallopolymer complexes were characterized using the automatic physisorption analyzer Micromeritics ASAP 2010, by the BET (Brunauer, Emmett-Teller) and BJH (Barrett−Joyner−Halenda) methods through N_2 adsorption−desorption. The metal ion dispersion and morphology of the chelating polymer and its complexes were recorded by scanning electron microscopy (SEM) using a JSM − 6300 (JEOL Co., Tokyo, Japan) electron microscope, operating at 20 kV with energy dispersive spectroscope (EDS) X-ray spectrometry (BRUKER AXS, Microanalysis GMBH, Berlin, Germany).

2.3. Synthesis of the Resin and Its Complexes. *2.3.1. Synthesis of Chlorosulphonated Polystyrene, $PsSO_2Cl$.* $PsSO_2Cl$ was synthesized following the method reported by Fish et al.[33] but after modification. Amberlite XAD-16 (5 g) in $CHCl_3$ (50 mL) was allowed to swell for 2 h then stirred with a mixture of chlorosulfonic acid ($ClSO_3H$; 50 mL) and chloroform ($CHCl_3$; 50 mL) for 24 h at room temperature, filtered off, washed thoroughly with dry dichloromethane (CH_2Cl_2), and dried in a vacuum at 60 °C for 72 h. The obtained polymer beads were refluxed in 50 mL $CHCl_3$ solution containing 25 mL thionyl chloride ($SOCl_2$) for 12 h to reduce $-SO_3H$ groups linked to polystyrene as a result of the hydrolysis of $-SO_2Cl$ when water is generated as a byproduct. The beads were filtered, washed and dried in the same fashion.

2.3.2. Synthesis of the Chelating Resin $PsSO_2ASA$. The chelating resin $PsSO_2ASA$ was synthesized by the reaction given in Scheme 1. The dry PS-SO_2Cl (5.0 g) was treated with 4-aminosalicylic acid (3.347 g) in acetone (20 mL). The reaction mixture was refluxed for 48 h and the product was filtered off, washed with acetone (3 × 15 mL) and diethyl ether (3 × 15 mL) and then dried under vacuum at 60 °C for 24 h.

2.3.3. Synthesis of the Metal Complexes. The pH of the solution of $Cu(NO_3)_2\cdot 2.5H_2O$, $Ni(NO_3)_2\cdot 6H_2O$, or $Co(NO_3)_2\cdot 6H_2O$; (0.1 mol L^{-1}) in double distilled water (100 mL) was adjusted to the pH range of 5.0 to 6.0 by adding the suitable buffer. The solid resin, $PsSO_2ASA$ (100 mg) was added and the reaction mixture was shaken for 8 h, filtered off, washed several times by ethanol (EtOH) and diethyl ether (Et_2O), and dried under vacuum at 60 °C for 48 h.

2.4. Recommended Methods for Preconcentration and Determination of the Metal Ions. *2.4.1. Column Method.* A glass column C10/10 (Pharmacia, 10 cm × 10 mm) was used for the present work. 500 mg of the dry $PsSO_2ASA$ was immersed in double distilled water and allowed to swell for 24 h by loading between frits, using the method recommended by the manufacturer. The column was treated with 30 mL of 2.0 mol L^{-1} HNO_3 solution and then rinsed with doubly distilled water until acid free. A suitable aliquot of the sample solution containing (10 to 50) mg L^{-1} of Cu(II), Ni(II), or Co(II) was passed through the column after adjusting its pH to the optimum value between 2.00 and 9.00 for Cu(II), Ni(II), and Co(II) at a flow rate (1.0 to 6.0) min^{-1} which was controlled by a peristaltic pump. The column was washed with distilled water to remove the free metal ions. The adsorbed metal ions were stripped from the column with 2.0 mol L^{-1} HNO_3 [(20 to 30) mL] passed at a flow rate of (1.0 to 6.0) mL min^{-1}. The concentration of the metal ions in the eluent was determined by ICP-AES.

2.4.2. Batch Method

2.4.2.1. Dosage of the Chelating Resin. The effect of $PsSO_2ASA$ amount (in the range of (100 to 700) mg was investigated for the uptake of Cu(II), Ni(II), and Co(II) ions by using an initial metal ion concentration (C_0) in the range of (50 to 300) mg L^{-1}. The percentage sorption was increased up to 500 mg of the resin after which it declined with increasing mass of chelating resin. Thus 500 mg of the chelating resin was used for the studies.

2.4.2.2. Effect of Shaking Time. The metal capacity was determined in triplicate by the batch method at pH 5.1 for Cu(II) and 6.0 for Ni(II) and Co(II) ions. To a 500 mL solution of the metal ion with initial concentration C_0 = 150 mg L^{-1} in a 1000 mL stoppered glass bottle was added 500 mg of $PsSO_2ASA$. The mixture was shaken at a constant shaking rate of 200 rpm at 298 K. The aqueous samples were taken at preset time intervals [(2 to 90) min] and the concentrations of metal ions were similarly measured by ICP-AES. The amount of adsorption at time t, (q_t, mg g^{-1}), was calculated from eq 1

$$q_t = (C_0 - C_t)V/m \quad (1)$$

where q_t is the amount of adsorbed metal ion at time t, C_0 and C_t (mg L^{-1}) are the initial concentration and the metal ion concentration remaining in aqueous solution at time t, respectively, V is the volume of the solution (L), and m is the mass of the chelating resin (g).

2.4.2.3. Effect of Initial Metal Ion Concentration and Temperature on the Metal Capacity. In order to evaluate the equilibrium isotherm model for the adsorption of Cu(II), Ni(II), and Co(II) ions, the experiments were conducted by placing 500 mg of the resin to 500 mL solutions in initial concentrations [(10 to 300) mgL^{-1}] of Cu(II), Ni(II), and Co(II) which were adjusted to pH 5.1 for Cu(II) and 6.0 for Co(II) and Ni(II) in a stoppered glass bottle (250 mL). The mixture was shaken for 120 min at 25 °C using an electrical shaker with a shaking rate of 200 rpm to reach equilibrium. A similar procedure was followed for another two sets of stoppered glass bottles under the same conditions but at (35 and 45) °C for thermodynamic studies. The resin was filtered off and washed several times with double distilled water. The filtrate and washings were collected in 250 mL, the solution was made up to the mark with double distilled water, and the residual metal ion concentration in the aqueous solution in each case was determined by using ICP-AES.

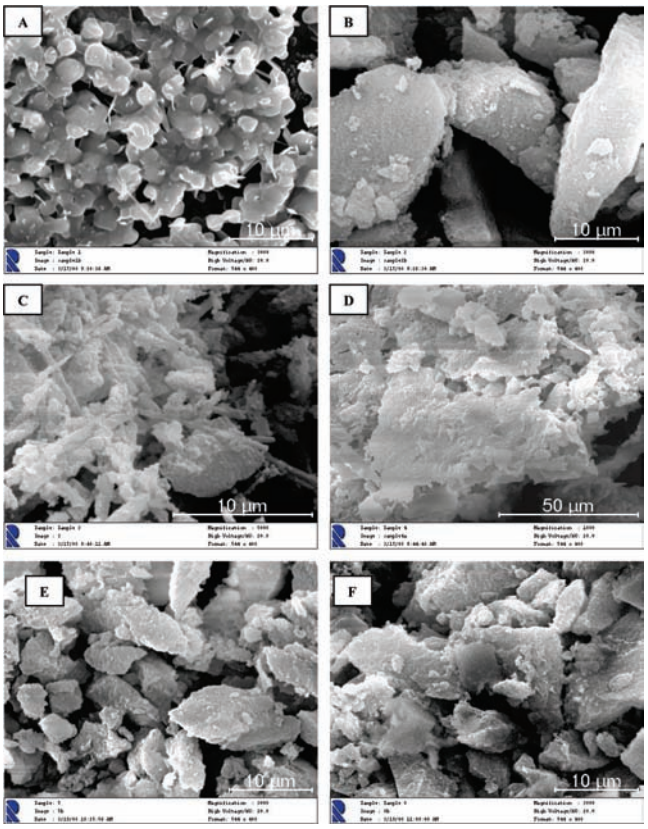

Figure 1. SEM micrographs of (A) Ps, (B) $PsSO_2Cl$, (C) $PsSO_2ASA$, (D) Cu-$PsSO_2ASA \cdot nH_2O$, (E) Co-$PsSO_2ASA \cdot nH_2O$, and (F) Ni-$PsSO_2ASA \cdot nH_2O$.

The amount of Cu(II), Ni(II), or Co(II) uptake at equilibrium q_e (mg g^{-1} resin) was calculated using eq 1.

3. RESULTS AND DISCUSSION

3.1. Characterization of the Chelating Resin and Its Complexes. *3.1.1. Elemental Analysis and Surface Studies.* $PsSO_2Cl$ was synthesized as reported by Fish et al.[33] and enhanced by our group.[23] Elemental analysis results of $PsSO_2Cl$ showed C = 47.39 %, H = 5.44 %, and S = 13.15 %. Calculated results for $C_{10}H_9SO_2Cl.H_2O$ are C = 48.68 %, H = 4.46 %, and S = 12.98 % showing 98 % sulfonyl chloride (4.66 mmol/g) and residual sulfonic acid (0.07 mmol/g). The $PsSO_2ASA$ was synthesized according to the reaction given in Scheme 1. The CHNS analyses, SEM (Figure 1) and EDS (Figure 2) of the resin have been compared to the free Amberlite XAD-16 and chlorosulfonated Amberlite XAD-16 indicating the formation of $PsSO_2ASA$. Elemental analysis showed C = 44.19 %, H = 5.08 %, N = 3.86 %, and S = 8.19 %. Calculated results for $C_{15}H_{13}NSO_5 \cdot 3.5H_2O$ are C = 47.12 %, H = 5.23 %, N = 3.66 %, and S = 8.37 %. The calculated % conversion of the chlorosulfonated polystyrene to the desired adsorbent of 98 % and the amount of chelating ligand incorporated (2.48 mmol g^{-1}, based on the nitrogen content) resin are also taken as evidence for the formation of $PsSO_2ASA$. This result also corresponds to the data similarly reported for the *N*-sulfonylethylenebis-(dithiocarbamate) ligand anchored on macroporous polystyrene-divinyl benzene beads[33] and *N*-sulfonylpolyamine chelating resins anchored on polystyrene-divinyl benzene beads.[24]

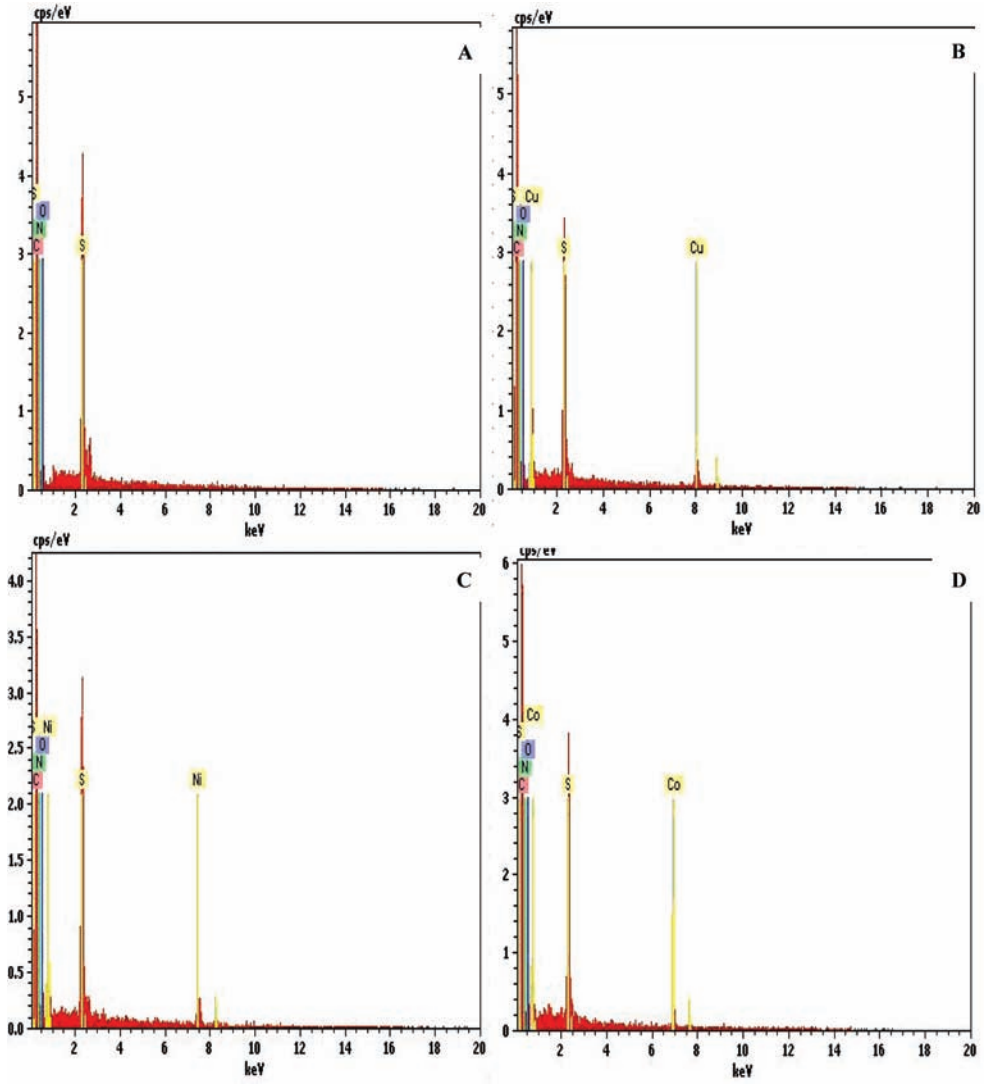

Figure 2. EDS analysis for (A) $PsSO_2ASA \cdot 3.5H_2O$, (B) Cu-$PsSO_2ASA \cdot nH_2O$, (C) Co-$PsSO_2ASA \cdot nH_2O$, and (D) Ni-$PsSO_2ASA \cdot nH_2O$.

The determined BET surface area ($m^2\ g^{-1}$), BJH cumulative pore volume ($cm^3\ g^{-1}$) and average pore diameter (4 V/A by BET), of the chelating resin have been found to be (99.593, 0.172, and 6.207) nm, respectively, less than those of the chlorosulfonated and free Amberlite XAD-16 which indicates the incorporation of the 4-aminosalicylic acid to chlorosulfonated Amberlite XAD-16. This may be attributed to formation of intra- and intermolecular hydrogen bonding. This incorporation is also proved from the EDS measurements (Figure 2). Furthermore, the EDS exhibits peaks characteristic of Cu, Ni, and Co supporting their absorption by the resin.

3.1.2. Infrared Spectral Studies. The FT-IR spectrum of the free $PsSO_2ASA \cdot 3.5H_2O$, exhibits a very strong broad band at 3434 cm^{-1} and a medium one at 3019 cm^{-1} due to $\nu_{(OH)}$ of adsorbed water and the salicylic moiety. The bands at (1662, 1384, and 1328) cm^{-1}, are assigned to $\nu_{(COO)asym}$, $\nu_{(COO)sym}$, and $\nu_{(C-O)phenolic}$,[34] respectively. These in addition to a strong one at 1620 cm^{-1} which could be assigned to $\nu(C{=}C)$. The FT-IR spectra of all complexes, exhibit a downward shift with a reduction in the intensities of the bands at (1662 and 1384) cm^{-1} with $\Delta\nu$ = (269, 276, and 275) cm^{-1}[34] for Cu(II), Ni(II), and Co(II) complexes, respectively, suggesting a monodentate bonding of the carboxylato-O atom to the metal ion. Furthermore, the band at 1328 cm^{-1} characteristic $\nu_{(C-O)phenolic}$ shifted to lower wave numbers suggesting the bonding of the phenolato-O atom to the metal ion. Accordingly, IR data in addition to the EDS confirm that the metal sorption by the chelating resin is due to the formation of metal complexes through coordination to the carboxylato-O and phenolato-O atoms as shown in Figure 3.

3.1.3. Thermogravimetric Analysis. Results of thermogravimetric analyses (TG and DTG) of $PsSO_2ASA$ and its metal complexes are shown in Figure 4 and the data given in Table 2. This data showed that the free chelating resin, $PsSO_2ASA$, (Figure 4a) exhibits an endothermic peak at 99.38 °C corresponding to the loss of $3.5H_2O$ of hydration. The dry resin is then completely decomposed between (222.56 to 450.00) °C in three stages without leaving solid residue.

The thermal stability data for metallopolymer complexes is important to confirm the presence of metal ions, either as inclusion complexes or as adsorbed species. Metal ions present as inclusion complexes are expected to have greater effects on the thermal properties of the chelating resins.[35−37] Furthermore, the

dx.doi.org/10.1021/je1008087 |*J. Chem. Eng. Data* 2011, 56, 1827–1839

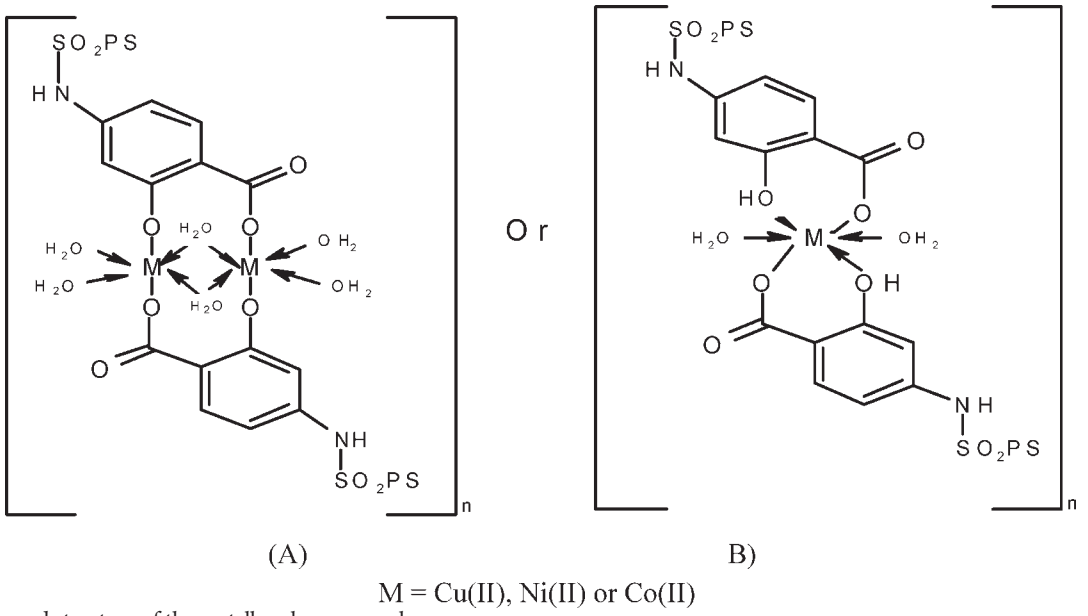

Figure 3. Assumed structure of the metallopolymer complexes.

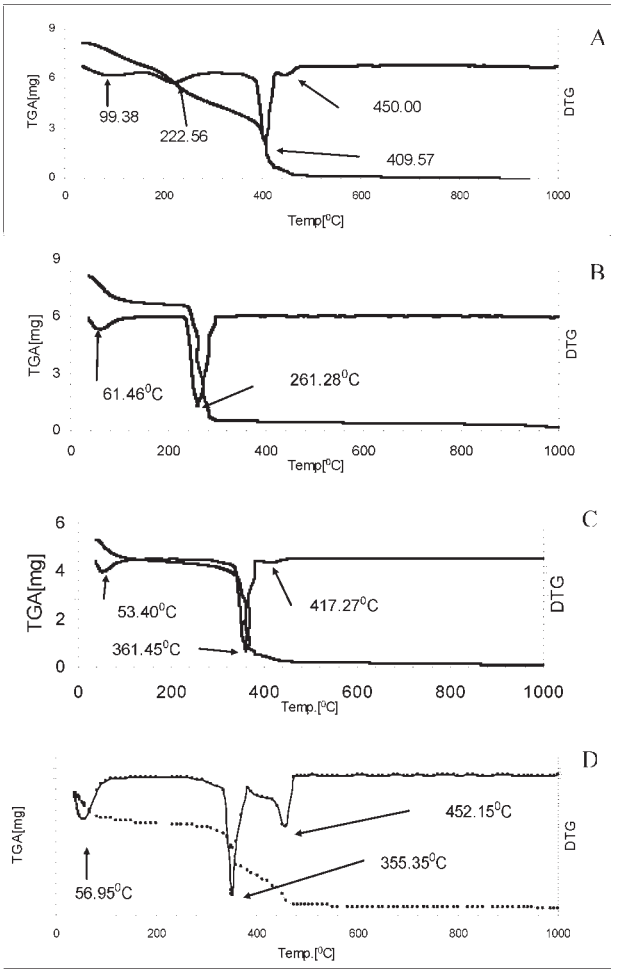

Figure 4. TGA and DTG of (A) $PsSO_2ASA \cdot 3.5H_2O$, (B) Cu-$PsSO_2ASA \cdot nH_2O$, (C) Co-$PsSO_2ASA \cdot nH_2O$, and (D) Ni-$PsSO_2ASA \cdot nH_2O$.

thermal stability of the metallopolymer complexes depends on the structure of the resin, mode of complexation and the structure of the metallopolymer complex[35−37] which may increase or decrease the thermal stability of the resin.

Accordingly, TG and DTG of the metal-$PsSO_2ASA$, Figure (4b-d) have been compared with the thermal behavior of the free chelating resin $PsSO_2ASA$, (Figure 4a). In all complexes the first peak due to the loss of physically adsorbed water appeared below 100 °C (Table 1). The thermal degradation obtained can be summarized in the following points: (i) The data given in Table 2 and shown in Figure (4a−d) indicated that in all cases the formation of metallopolymer complexes increased the thermal stability of the resin. This also suggests complex formation due to the formation of additional chemical bonds and interaction between the metal ions and the ligand group through the interpolymer chain. (ii) The thermal stability is seen in the order of: Co-$PsSO_2ASA \cdot nH_2O$ > Ni-$PsSO_2ASA \cdot nH_2O$ > Cu-$PsSO_2ASA \cdot nH_2O$ > $PsSO_2ASA \cdot nH_2O$. (iii) The resin decomposes in a single step in Co-$PsSO_2ASA \cdot nH_2O$ and Cu-$PsSO_2ASA \cdot nH_2O$ while it decomposes in two separate steps in the case of Ni-$PsSO_2ASA \cdot nH_2O$. (iv) The lowest thermal stability of the copper metallopolymer complex may refer to the highest complexing ability of the resin for Cu(II) as compared to the other two metal ions in accordance with the kinetic and equilibrium data.

3.1.4. Electronic and ESR Spectral Studies of the Complexes. The nujol mull electronic spectrum of the Cu(II) complex displays a broad band at 16150 cm^{-1} with low intensity. The band position and shape is consistent with a d-d transition in a tetragonally distorted Cu(II) complex. The room temperature ESR spectrum of the polycrystalline Cu(II) complex is shown in Figure 5. The spectrum consists of three signals characteristic of a rhombic system which gives three *g*-values of 2.38, 2.08, and 2.06 for g_z, g_y, and g_x, respectively. This, in addition to a weak signal at 1626 G (half field region, $g = 4.25$) due to $\Delta M_s = \pm 2$, forbidden transition characteristic of polymeric Cu(II) complexes. The very low intensity of this signal indicates that the Cu−Cu separation distance is more than 5 Å and the zero field splitting is very small. The value of g_z (g_{11}) = 2.38 indicates the ionic nature of the Cu-ligand bond and confirms that the $d_{x^2-y^2}$ is most popular in the ground state.[23] Taking $g_\perp = {}^1/_2[g_y + g_x] = 2.07$, the value of the

dx.doi.org/10.1021/je1008087 |J. Chem. Eng. Data 2011, 56, 1827–1839

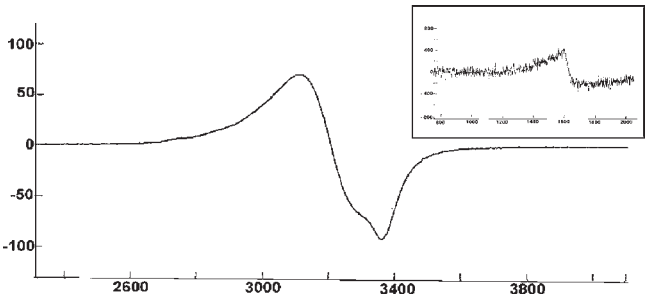

Figure 5. Room temperature X-band ESR spectrum of a polycrystalline Cu-$PsSO_2ASA \cdot nH_2O$.

Table 1. Main IR Bands (ν, cm^{-1}) of the Chelating Resin ($PsSO_2ASA$) and Its Metal Complexes with Their Tentative Assignments

compound	$\nu_{(NH)}$ and $\nu_{(OH)}$	$\nu_{(COO)}$-asym	$\nu_{(COO)}$-sym	$\nu_{(C-O)}$-phenolic
$PsSO_2ASA \cdot 3.5H_2O$	3434.3019	1662	1384	1328
Cu- $PsSO_2ASA \cdot nH_2O$	3445.3148	1634	1365	1269
Ni- $PsSO_2ASA \cdot nH_2O$	3380.3255	1647	1371	1278
Co- $PsSO_2ASA \cdot nH_2O$	3368.3220	1649	1374	1278

Table 2. Thermoanalytical Results of $PsSO_2ASA$ and Its Metal Complexes

	TG	DTG	weight loss	
compound	T_{range}/°C	T_{max}/°C	%	% residue
$PsSO_2ASA \cdot 3.5H_2O$	42.12−151.33	99.38	16.003	
	162.25−297.97	227.3	45.16	
	358.81−429.02	409.57	92.79	
	438.00−495.00	460.1	100.00	0. 00
Cu- $PsSO_2ASA \cdot nH_2O$	40.56−121.69	70.44	18.042	
	218.41−316.69	261.28	93.68	6.32
Ni- $PsSO_2ASA \cdot nH_2O$	39.02−117.01	61.75	11.90	
	296.41−374.42	355.35	59.91	
	382.22−494.54	459.8	94.91	5.09
Co- $PsSO_2ASA \cdot nH_2O$	43.68−102.96	60.02	17.61	
	316.69−388.46	359.7	91.33	
	390.02−463.34	422.9	94.72	5.28

exchange interaction parameter, $G = g_{11} - 2/g_{\perp} - 2 = 5.43$ can be calculated. This value indicates that the exchange interaction between the copper centers in the solid state could be neglected.

The hyperfine line splitting factor $A_{\parallel}$ of 176G G is obtained from the spectrum indicating the planarity of the complex. In general, the empirical factor $f = g_{\parallel}/A_{\parallel}$ is an index of the tetragonal distortion or the distortion toward the tetrahedral, and is calculated to be 135 cm^{-1}. The value is less than 150 cm^{-1}, the higher limit of the planar complexes and rather indicates a planar structure, may be due to the inflexible structure of the polymeric molecule. In general the distortion from planarity toward tetragonally distorted octahedral toward the tetragonally distorted octahedral or tetrahedral structure results in a decrease in $A_{\parallel}$ and increase in $g_{\parallel}$ as shown in a number of Cu(II) complexes. As shown, $A_{\parallel}$ is of moderate value and in line with that of dominantly planar complexes especially. The value of the in-planar π bonding parameter α^2 can be estimated from the expression

$$\alpha^2 = A_{\parallel}/0.036 + (g_{\parallel} - 2.0023) + 3/7(g_{\perp} - 2.0023) + 0.04$$

and is found to be 0.96 which is consistent with mainly ionic copper-in-plane-ligand bonding which is also in agreement with results obtained for the value of $g_{\parallel} > 2.30$.

The nujol mull electronic spectrum of the Ni(II) complex exhibits a broad band at 16 350 cm^{-1} in addition to a weak one at 10 900 cm^{-1}, characteristic of a tetragonally distorted octahedral ligand field. These bands could be assigned to $^3A_{2\,g}(F) \rightarrow {}^3T_{2\,g}(F)$, ν_3, $^3A_{2\,g}(F) \rightarrow {}^3T_{1\,g}(F)$, ν_2, transitions. The transition due to $^3A_{2\,g}(F) \rightarrow {}^3T_{1\,g}(P)$, ν_1, may be obscured by the intense band due to charge transfer.[23]

The spectrum of the Co(II) complex displays bands at (17 100 and 19 050) cm^{-1} consistent with an octahedral ligand field around the cobalt(II). These two bands could be assigned to $^4T_{1\,g} \rightarrow {}^4T_{2\,g}$ and $^4T_{1\,g} \rightarrow {}^4T_{1\,g}(P)$ transitions, and the absence of a band below 10 000 cm^{-1} may be due to its very low intensity.[23] The electronic and ESR spectral data are further evidence for complex formation rather than a physical adsorption mechanism. Based on the spectral data, and the nature of the resin, structure in Figure 3A could be assumed to be the most probable for the complexes.

Table 3. Optimum Experimental Parameters for the Sorption and Desorption of the Analytes

parameter	Cu(II)	Ni(II)	Co(II)
pH range	5.0−6.0	6.0−7.0	6.0−7.0
flow rate/(mL min^{-1})	2.0−4.0	2.0−4.0	1.5−5.0
HNO_3 desorption	2 mol L^{-1}	2 mol L^{-1}	2 mol L^{-1}
metal sorption capacity/(mg g^{-1})	28.643	15.312	19.155
lower limit detection/(ng mL^{-1})	20	10	10
breakthrough volume/(mL)	2000	1500	2000
final volume/(mL)	5	5	6
preconcentration factor (2.0 mol L^{-1} HNO_3)	400	300	333.3

3.2. Analytical and kinetic studies. The optimum experimental parameters for quantitative metal ion sorption and desorption are listed in Table 3. The effect of concentration of HCl and HNO_3 on the preconcentration of the metal ions was studied under these optimum conditions. The results in Table 4 show that the most suitable eluent is 2.0 mol L^{-1} HNO_3. Each experiment was performed in triplicate under the same conditions.

3.2.1. Effect of Initial pH on the Metal Capacity. The effect of initial pH on the sorption capacity of the chelating resin $PsSO_2ASA$, toward Cu(II), Ni(II), and Co(II) with initial concentrations C_0 = 150 mg L^{-1}, has been studied. The data show that the maximum adsorption for these metal ions occurred at pH 5.08 for Cu(II) and 6.0 for both Co(II) and Ni(II) with an adsorption amount of (28.643, 15.312, and 19.155) mg g^{-1}, respectively. The higher maximum adsorption capacity value of the resin for Cu(II) ions indicated that the complexation ability of Cu(II) with the chelating resin was higher as compared to both Co(II) and Ni(II). Furthermore, the difference in the maximum capacity indicates the ease of separation of copper ions from a mixture of Cu(II), Ni(II), and Co(II) ions. The acidity of the medium can affect the metal ion uptake by the resin because of

Table 4. Type of Eluent Solution and % Recovery (R.S.D.) of the Metal Ions, 10 mL Sample Volume with 0.5 mg mL^{-1} of Cu(II), Ni(II), or Co(II) and n = 3

eluent	Cu(II)	Ni(II)	Co(II)
0.1 mol L^{-1} HCl	28.0(3.8)	49.0(3.0)	27.0(2.1)
0.5 mol L^{-1} HCl	49.0(2.1)	54.0(1.9)	38.0(1.8)
1.0 mol L^{-1} HCl	74.0(3.9)	78.0(1.9)	65.0(1.7)
2.0 mol L^{-1} HCl	88.0(3.0)	83.0(2.3)	89.0(1.2)
3.0 mol L^{-1} HCl	96.0(2.1)	97.0(1.7)	98.0(2.2)
0.1 mol L^{-1} HNO_3	48.0(4.4)	52.0(2.7)	51.0(1.9)
0.5 mol L^{-1} HNO_3	61.0(4.3)	70.0(3.1)	72.0(3.9)
1.0 mol L^{-1} HNO_3	88.0(1.8)	80.0(2.5)	82.0(4.9)
1.5 mol L^{-1} HNO_3	90.0(3.8)	91.0(4.7)	93.0(2.2)
2.0 mol L^{-1} HNO_3	99.0(2.4)	99.0(2.8)	98.0 (3.4)
3.0 mol L^{-1} HNO_3	96.0 (2.7)	98.0(2.3)	95.0(2.5)

the competition of the high concentration of hydrogen ion at low pH with the metal ion for bonding to the active sites on the surface of the adsorbent, since the active sites on the chelating resin are the carboxylic and phenolic OH groups. At pH values higher than 7.00, the three metal ions may precipitate out as metal hydroxides which leads to an increase in metal uptake.[38−41]

3.2.2. Sorption Kinetics. The effect of shaking time on the sorption of Cu(II), Co(II), and Ni(II), (C_0 = 150 mg L^{-1}), at pH 5.08, 6.00 and 6.00, by $PsSO_2$-ASA (500 mg), respectively, at 298 K has been studied by the batch method. Complete saturation is reached after 30 min for Cu(II) and 40 min for Ni(II) and Co(II). The metal uptake capacity of the chelating resin has been found to be in the order: Cu(II) > Co(II) > Ni(II).

The kinetic models that were used to examine the controlling mechanisms of the sorption process based on the experimental data are:

(i) Pseudofirst order model (eq 2) given by Lagergren[41,42]

$$\log(qe - q_t) = \log q_e - k_1/2.303t \quad (2)$$

(ii) Pseudosecond order model (eq 3)[42,43]

$$t/q_t = 1/k2q_e^2 + t/q_e \quad (3)$$

and

(iii) Intraparticle diffusion model (eq 4) given by Weber and Morris[43,44] which is a common diffusion model that describes that metal ion uptake varies almost proportionally with $t^{0.5}$, rather than the contact time t

$$q_t = C + k_{int}t^{0.5} \quad (4)$$

where q_e and q are the amounts of the metal ions absorbed (mg g^{-1}) at equilibrium and at time t (min), respectively, k_1 (min^{-1}), k_2 (g mg^{-1} min^{-1}), and k_{int} (mg g^{-1} min$^{-1/2}$) are the first, second, and intraparticle diffusion rate constants, respectively, and C is the intercept of the straight line which is proportional to the boundary layer thickness.[44]

The kinetic parameters (Table 5) for the pseudofirst order and pseudosecond order models are obtained from linear plots of $\log(q_e - q)$ vs t (Figure 6A), t/q vs t (Figure 6B), and q vs $t^{0.5}$ (Figure 6C), respectively. The experimental q_e values for Cu(II), Ni(II), and Co(II) are in agreement with the calculated values

Table 5. Kinetic Parameters of the Sorption of Cu(II), Ni(II), and Co(II)

	q_e			
	mg g^{-1}		k_1	
pseudofirst order	exp	calc	min^{-1}	R^2
Cu(II)	28.643	28.262	0.0304	0.9661
Ni(II)	15.312	15.265	0.0316	0.9412
Co(II)	19.155	19.295	0.0279	0.9140

	q_e				
	mg g^{-1}		k_2	h	
pseudosecond order	exp	calc	g mg^{-1} min^{-1}	mg g^{-1} min^{-1}	R^2
Cu(II)	28.643	28.662	0.0030	5.737	0.9984
Ni(II)	15.312	15.365	0.0038	5.708	0.9986
Co(II)	19.155	19.195	0.0063	6.510	0.9979

	k_{id}	C	
	mg g^{-1} min$^{-0.5}$	mg g^{-1}	
intraparticle diffusion			R^2
Cu(II)	13.243	3.617	0.9336
Ni(II)	13.243	3.694	0.8543
Co(II)	12.289	2.626	0.8717

(Table 5) using the pseudosecond order and pseudofirst order kinetic models. Based on the values of the coefficients of determination, R^2 and the values of q_e (Table 5), the pseudosecond order equation is the model that best fits the experimental kinetic data, suggesting chemical sorption as the rate determining step. A similar phenomenon has been observed in the adsorption of many trace metal ions by different chelating resins.[45−51] Accordingly, the adsorption of Cu(II), Ni(II), and Co(II) ions by $PsSO_2$ASA is considered to consist of two processes with initial adsorption rates (h) of (5.737, 6.510, and 5.707) mg g^{-1} min^{-1} for Cu(II), Ni(II), and Co(II), respectively, which have been calculated by using eq 5.

$$h = k_2q_e^2 \quad (5)$$

The carboxylic and hydroxyl groups on the surface of $PsSO_2$A-SA are responsible for metal ion binding through a coordination mechanism as proved from the solid complex studies. Physical adsorption plays a negligible role in the interaction mechanism between $PsSO_2$ASA and the metal ion because the chelating resin has a small surface area of 99.593 m^2 g^{-1}. This data is very similar to that reported for several chelating resins with a small surface area as thiourea-modified magnetic chitosan micropores,[49,50] macromolecular complexes with polystyrene and acrylic acid[51] and polystyrene-*N*,*N*′-di(carboxymethyl)dithiocarbamate chelating resin.[51]

The intraparticle diffusion model has also been utilized to determine the rate limiting step of the adsorption process. Therefore, the sorbed concentration at time t (q_t) was plotted against $t^{0.5}$ to test the Morris-Weber equation (eq 4). The plot

dx.doi.org/10.1021/je1008087 |*J. Chem. Eng. Data* 2011, 56, 1827–1839

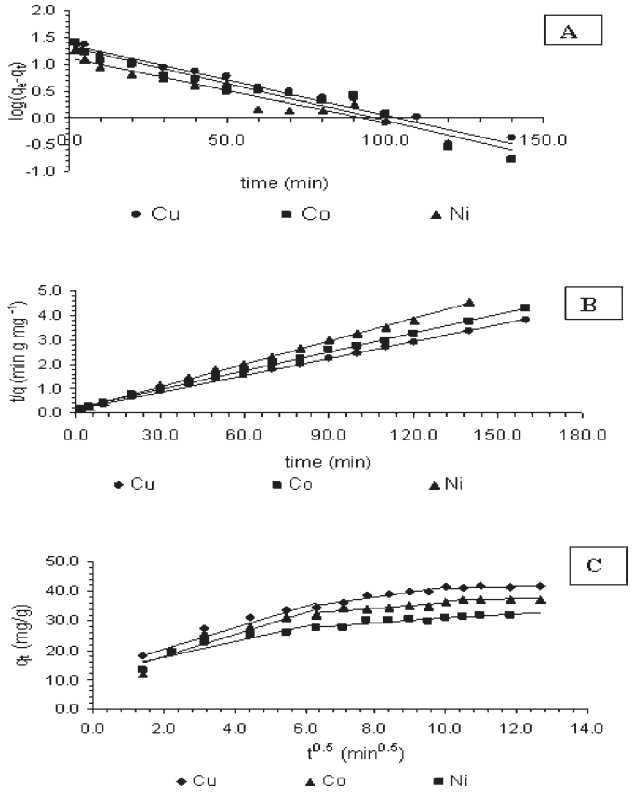

Figure 6. (A) Pseudo first order sorption kinetics of Cu(II), Ni(II), and Co(II) at pH (5.08, 6.00, and 6.00), respectively by the chelating resin $PsSO_2ASA$, T = 298 K, m = 500 mg. (B) Pseudo second order sorption kinetics of Cu(II), Ni(II), and Co(II) at pH (5.08, 6.00, and 6.00), respectively by the chelating resin $PsSO_2ASA$, T = 298K, m = 500 mg. (C) Uptake of Cu(II), Ni(II), and Co(II) ions by $PsSO_2ASA$ as a function of $t^{1/2}$.

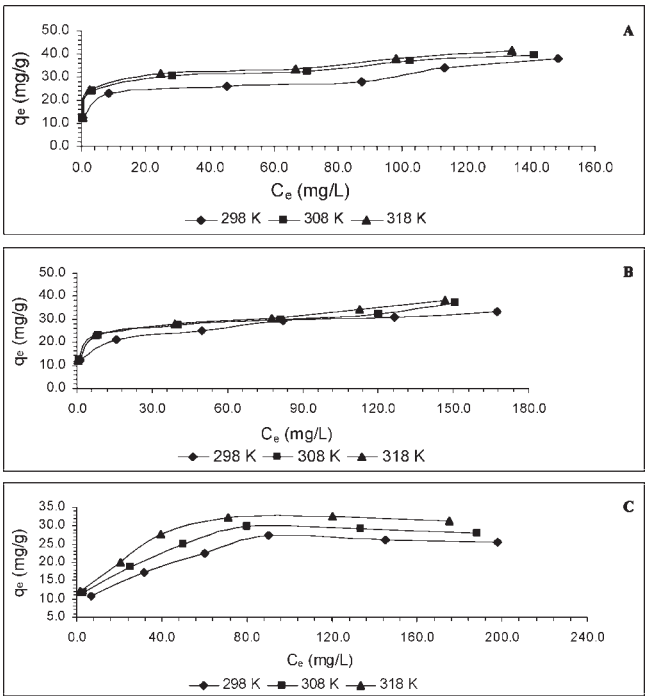

Figure 7. (A) Equilibrium adsorption isotherm of Cu(II) with C_0 = (50, 100, 150, 200, 250, and 300) mg/L, T = (298, 308, and 318) K, m = 500 mg resin, shaking rate = 200 rpm, shaking time = 120 min, and pH value of 5.08. (B) Equilibrium adsorption isotherm of Co(II) with C_0 = (50, 100, 150, 200, 250, and 300) mg/L, T = (298, 308, and 318) K, m = 500 mg resin, shaking rate = 200 rpm, shaking time = 90 min, and pH value of 6.00. (C) Equilibrium adsorption isotherm of Ni(II) with C_0 = (50, 100, 150, 200, 250, and 300) mg/L, T = (298, 308, and 318) K, m = 500 mg resin, shaking rate = 200 rpm, shaking time = 90 min, and pH value of 6.00.

(Figure 6C) showed three portions; the first of which is sharper and obtained between (30 to 39) min, in which eq 5 held with regression coefficients of 0.9694−0.9954 and values of k_{int} of (13.243, 13.241, and 12.241) mg/g $min^{0.5}$ for Cu(II) Ni(II), and Co(II), respectively, were obtained from the slope of each plot. This portion represents the diffusion of the metal ion through the solution to the external surface of adsorbent or boundary layer diffusion of solute ions. The second portion represents the gradual adsorption stage where intraparticle diffusion is rate limiting. The third portion is the final equilibrium stage where intraparticle diffusion starts to slow down due to the extremely low metal ion concentrations left in solution. It has been reported that if intraparticle diffusion occurs, q_t versus $t^{0.5}$ will be linear and if the plot passes through the origin, then the rate limiting step is only due to intraparticle diffusion.[49] Other mechanisms in addition to the intraparticle model have been tried. Therefore, in this study, the intraparticle diffusion is applied but is not the only rate limiting step in the adsorption process. Furthermore, the values of C of (3.617, 3.694, and 2.626) mg/g and k_{int} of (13.243, 13.243, and 12.289) mg/g $min^{0.5}$ for Cu(II), Ni(II), and Co(II), respectively, support the boundary layer diffusion effect.

3.2.3. Adsorption Isotherms. The equilibrium isotherm relationship between the amount of metal exchanged q_e and the remaining metal ion concentration in the aqueous phase (C_e) for the interaction between $PsSO_2ASA$ and Cu(II), Ni(II), and Co(II) ions are shown in Figure.7. It is shown that the sorption capacity increases with the equilibrium concentration of the metal ion in solution, progressively saturating the adsorbent. Also, it is shown that the metal sorption is more sensitive at low metal ion concentrations up to 25 mg L^{-1}. Therefore, this electrostatic interaction plays an important role in the coordination between the metal ions and the coordinating groups (−COOH and −OH). On the other hand, at higher concentrations, the sorption becomes relatively insensitive, although the resin displays high affinity toward the metal ion indicating that the sorption is mainly due to chelating interactions.

The effect of temperature on the metal uptake (Figure 7) shows that the metal sorption increases with increasing temperature indicating that the sorption is an endothermic process. Furthermore, this behavior can be attributed to (i) the number of coordinating sites on the resin surface which are increased due to partial dehydration, (ii) dehydration of the metal ions, and (iii) the possibility of enlargement of pores with increasing temperature which leads to an increase in diffusion of the metal ion toward the active sites in these pores.

To evaluate the sorption capacity of $PsSO_2ASA$ for removal of Cu(II), Ni(II), and Co(II), the Langmuir[53] and Freundlich[54] isotherm models have been used.

The Langmuir model could be presented as eq 6

$$C_e/q_e = 1/(K_L q_m) + C_e/q_m \quad (6)$$

where q_e (mg g^{-1}) is the amount of the metal ion adsorbed per unit mass of adsorbent and C_e (mg L^{-1}) is the equilibrium metal

ion concentration in aqueous solution. K_L (L g^{-1}) is the Langmuir constant which is related to the energy of sorption and q_m (mg g^{-1}) is the maximum adsorption capacity for the monolayer formation on the absorbent. A plot of c_e/q_e against C_e at different temperatures for each metal ion gives straight lines (Figure 8) from which the values of K_L and q_m have been estimated (Table 6).

The values of correlation coefficient and q_m obtained from the Langmuir plots at 298 K (room temperature) are comparable to those experimentally obtained, indicating that the sorption process is mainly a monolayer. Furthermore, the values of q_m at different temperatures are in the order Cu(II) > Co(II) > Ni(II) which is in agreement with the order observed in the kinetic studies.

The degree of suitability of the chelating resin toward the metal ion is estimated from the value of the separation factor R_L which describes the possibility of the adsorption process to proceed and has been determined by using eq 7

$$R_L = 1/(1 + K_L C_0) \quad (7)$$

where K_L is the Langmuir constant and C_0 is the initial concentration of the metal ion (mg L^{-1}).[55] In general, R_L >1.0 indicates the unsuitability of the resin: R_L = 1 means a reversible process, R_L = 0 indicates an irreversible process, and 1 > R_L > 0 indicates the suitability of the resin for sorption processes. The values of R_L for Cu(II), Ni(II), and Co(II) at different temperatures are in the range of 0.02−0.25, indicating the suitability of $PsSO_2ASA$ for the sorption of the studied metal ions from aqueous solutions.

The experimental data also fit the Freundlich expression[52] eq 8

$$\log q_e = \log K_F + (1/n) \log C_e \quad (8)$$

where K_F is the Freundlich constant (mg g^{-1}) and $(L/mg)^{1/n}$, where $1/n$ is the heterogeneity factor, are related to the energy or intensity of sorption. Plots of log q_e versus log C_e at different temperatures for each metal ion are shown in Figure 9. From the straight lines obtained, the values of K_F and n are estimated and are given in Table 6. The values of R^2 indicate that Langmuir model is more suitable than the Freundlich expression.

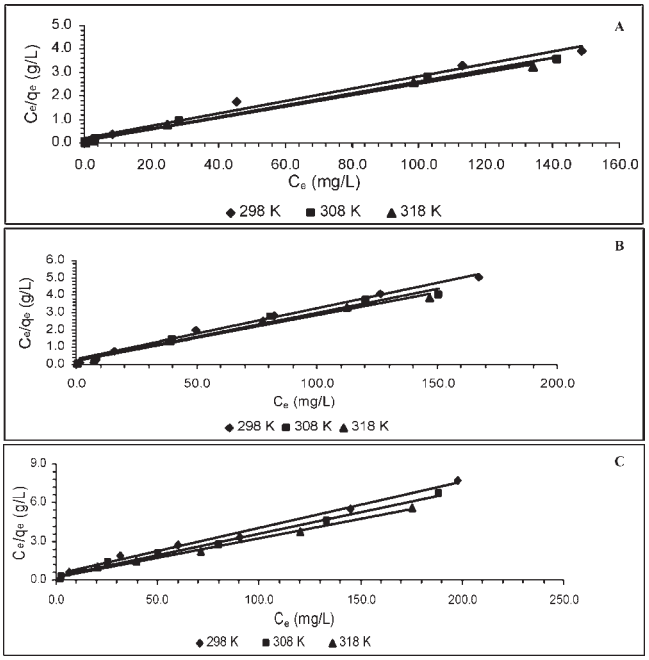

Figure 8. (A) Langmuir isotherm plot for adsorption of Cu(II) at T = (298, 308, and 318) K. (B) Langmuir isotherm plot for adsorption of Co(II) at T = (298, 308, and 318) K. (C) Langmuir isotherm plot for adsorption of Ni(II) at T = (298, 308, and 318) K.

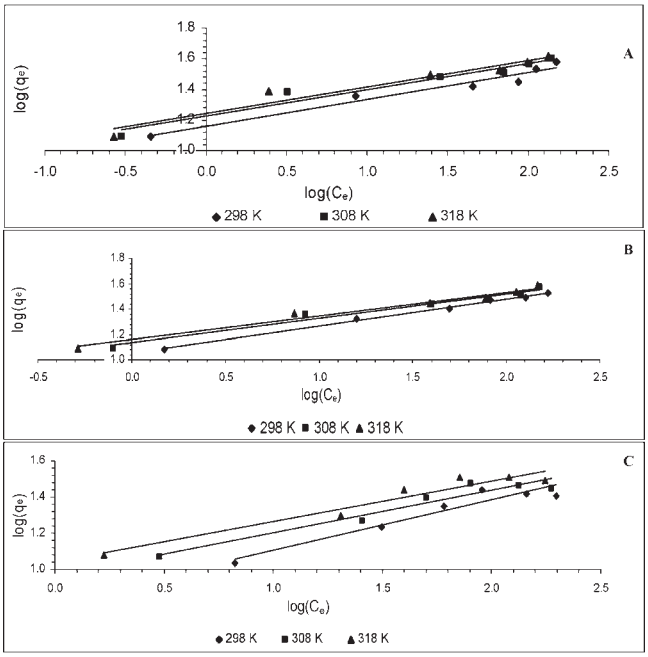

Figure 9. (A) Freundlich isotherm plot for adsorption of Cu(II) at T = (298, 308, and 318) K. (B) Freundlich isotherm plot for adsorption of Co(II) at T = (298, 308, and 318) K. (C) Freundlich isotherm plot for adsorption of Ni(II) at T = (298, 308, and 318) K.

Table 6. Freundlich and Langmuir Parameters of the Sorption of Cu(II), Ni(II), and Co(II)

		Cu(II)			Co (II)			Ni(II)		
isotherm	parameters	298 K	308 K	318 K	298 K	308 K	318 K	298 K	308 K	318 K
Freundlich	$1/n$	0.175	0.172	0.174	0.211	0.192	0.186	0.279	0.235	0.226
	n	5.717	5.810	5.753	4.748	5.200	5.380	3.573	4.253	4.418
	$k_F/(mgg^{-1})$ $(Lmg^{-1})^{1/n}$	14.457	16.815	17.466	11.318	13.536	14.501	6.658	9.255	10.911
	R^2	0.955	0.953	0.945	0.995	0.969	0.978	0.924	0.932	0.944
Langmuir	$q_{max}/(mgg^{-1})$	38.167	39.682	41.152	34.013	36.363	37.878	27.855	29.761	32.894
	$K_L/(L/g)$	0.119	0.259	0.279	0.099	0.122	0.124	0.083	0.136	0.160
	R^2	0.983	0.995	0.995	0.992	0.981	0.982	0.992	0.993	0.995

dx.doi.org/10.1021/je1008087 |J. Chem. Eng. Data 2011, 56, 1827–1839

3.2.4. Thermodynamics of Sorption. The effect of temperature on the sorption of Cu(II), Ni(II), and Co(II) ion onto the chelating resin, $PsSO_2ASA$ has been studied over the temperature range of (298 to 318) K under optimum conditions. A linear plot has been obtained by plotting log K_d (distribution coefficient = q_e/c_e,) against $1/T$ (Figure 10). The plot indicates that the values of K_d increase with increasing temperature which is a further indication of the endothermic sorption process. The values of the thermodynamic parameters such as Gibbs energy (ΔG), enthalpy (ΔH), and entropy (ΔS) are estimated using the relations 9−11

$$\Delta G = -RT \ln K_d \quad (9)$$

$$\Delta G = \Delta H - T\Delta S \quad (10)$$

$$\log K_d = (\Delta S/2.303R) - (\Delta H/2.303RT) \quad (11)$$

where K_d is the distribution coefficient and R is the universal gas constant (8.314 J mol^{-1} K^{-1}) and T is the absolute temperature (K). Plotting log K_d against $1/T$ (Figure 10) gives a straight line with slope = $-\Delta H/2.303R$ and intercept = $\Delta S/2.303R$ from which the values of ΔH and ΔS have been calculated and are given in Table 7. The positive values of ΔH indicate an endothermic chemical sorption of Cu(II), Ni(II), and Co(II).[18] The negative values of ΔG for the three metal ions indicate that the metal sorption was spontaneous and thermodynamically favorable. More negative ΔG implies a greater driving force of adsorption, resulting in higher sorption capacity. The data (Table 7) showed that (i) the values of ΔG become more negative with increasing temperature indicating that the sorption processes become more favorable and easier at higher temperatures and (ii) the values of ΔG are more negative in the order: Cu(II) > Co(II) > Ni(II) in all temperature ranges implying that the sorption is spontaneous and easier in the same sequence. The positive values of ΔS are also attributed to the liberation of

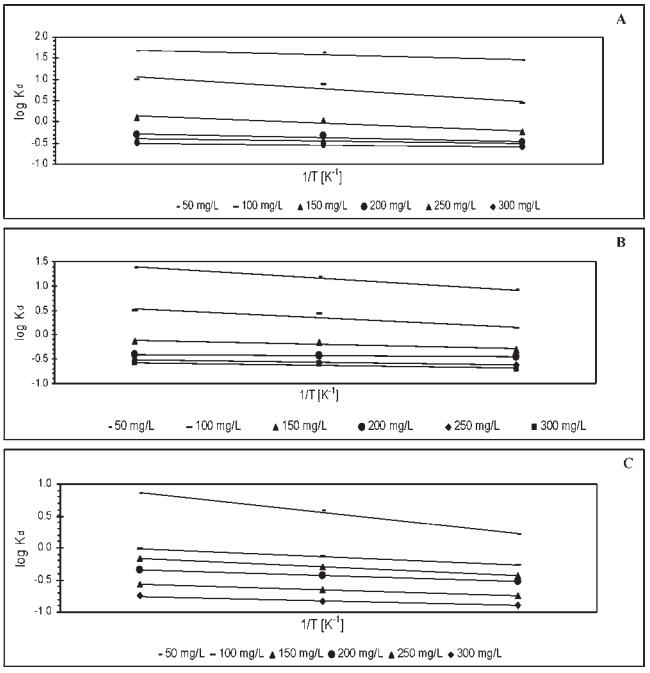

Figure 10. (A) Van't Hoff plots for sorption of Cu(II) ions with initial concentrations (50, 100, 150, 200, 250, and 300) mg L^{-1}. (B) Van't Hoff plots for sorption of Co(II) ions with initial concentrations (50, 100, 150, 200, 250, and 300) mg L^{-1}. (C) Van't Hoff plots for sorption of Ni(II) ions with initial concentrations (50, 100, 150, 200, 250, and 300) mg L^{-1}.

Table 9. Determination of Cu(II), Ni(II), and Co(II) in μg L^{-1}, (R.S.A.) in Tap Water Samples Using $PsSO_2ASA$[a]

sample	method	Cu(II)	Ni(II)	Co(II)
Kuwaiti tap water	direct	14.8(0.6)	6.8(1.2)	13.8(1.0)
	S.A.	115.0(1.0)	107.1(1.1)	114.0(0.9)
gulf water	direct	154.0(1.4)	105.6(2.8)	98.5(2.6)
	S.A.	254.7(1.2)	206.0(1.0)	198.9(1.1)

[a] SA = standard addition method (spikled with 100 μg L^{-1} solution of analyte).

Table 7. Thermodynamic Parameters for Sorption of Cu(II), Co(II), and Ni(II) at C_0 = 50 and 100 mg/L[a]

C_0	Cu(II)				Ni(II)				Co(II)			
mg L^{-1}	ΔH^0	ΔS^0	$-\Delta G^0$	R^2	ΔH^0	ΔS^0	$-\Delta G^0$	R^2	ΔH^0	ΔS^0	$-\Delta G^0$	R^2
50	20.89	97.99	8.308	0.90	42.43	160.0	5.25	0.992	58.88	201.86	1.275	0.999
			9.289				6.86				3.290	
			10.26				8.46				5.310	
100	52.22	184.3	2.72	0.91	34.08	117.4	0.92	0.889	23.18	72.72	1.513	
			4.56				2.09				0.786	
			10.26				3.27				0.058	0.999

[a] ΔH^0/(kJ mol^{-1}); ΔS^0/(J mol^{-1} K^{-1}); ΔG^0/(kJ mol^{-1}).

Table 8. Enrichment Factors and Enrichment Limits of the Metal Ions

	total volume	lower concentration	recovery	final volume	recovery	
metal ion	mL	ng mL^{-1}	ngmL^{-1} (R.S.D.)	mL	%	preconcentration factor
Cu(II)	2000	20.0	19.90(2.1)	5	99.5	400.0
Ni(II)	1500	10.0	9.61(1.2)	5	96.1	300.0
Co(II)	2000	10.0	9.81(0.8)	6	98.4	333.3

dx.doi.org/10.1021/je1008087 |J. Chem. Eng. Data 2011, 56, 1827–1839

Table 10. Comparison of Sorption Capacity of PsSO2ASA and Other Chelating Resins

matrix: chelating resin	Cu(II)	Ni(II)	Co(II)	ref
1. Sorption Capacities/(μ mol g^{-1})				
AnberliteXAD-16: gallic acid	344	250	281	54
Amberlite XAD-16: 2-{[1-(3,4-dihydroxyphenyl)methylidene]amino}benzoic acid	468	269	221	21
AnberliteXAD-16: 4-{[2-hydroxyphenyl)iminomethyl}-1,2-benzenediol	415	225	245	55
AnberliteXAD-16: 1,3-dimethyl-3-aminopropan-1-ol	460	550	270	4
AnberliteXAD-16: 1-(2-pyridylazo)2-naphthol	78	-	79	56
AnberliteXAD-16: calyx[4] resorcinarene	97.4	97.6	95.6	57
AnberliteXAD-16: 4-aminosalicylic acid (this work)	601	473	580	
2. Preconcentration Factors				
AnberliteXAD-16: gallic acid	400	300	285.7	54
Amberlite XAD-16: 2-{[1-(3,4-dihydroxyphenyl)methylidene]amino}benzoic acid	300	100	167	21
AnberliteXAD-16: 4-{[2-hydroxyphenyl)iminomethyl}-1,2-benzenediol	250	250	300	55
AnberliteXAD-16: 1,3-dimethyl-3-aminopropan-1-ol	400	300	300	4
AnberliteXAD-16: 1-(2-pyridylazo)2-naphthol	200		200	56
AnberliteXAD-16: calyx[4] resorcinarene	208	208	208	57
AnberliteXAD-16: 4-aminosalicylic acid (this work)	400	300	333	

hydrogen ions from the chelating resin, water of hydration of the metal ions and adsorbed water by the chelating resins and/or the degree of freedom increased at the solid−liquid interface during the sorption of the metal ions onto $PsSO_2ASA$.

3.2.5. Resin Stability and Reusability. The stability of the Ps-SO_2ASA chelating resin has been studied in (1.0 to 6.0) mol L^{-1} HCl or HNO_3. The chelating resin has been shaken in an acid solution of varying concentrations for 6 h at 25 °C and filtered. The resin was washed with distilled water until it was acid free and dried under vacuum at 60 °C for 24 h. The sorption capacity of the acid treated resin is found to be similar to the untreated one but with a variation of (2 to 3) %. This indicates that Ps-SO_2ASA can be stable in acid medium up to 6.0 mol L^{-1}. Furthermore, it is shown that this resin can be reused for 25 cycles of sorption−desorption with a (2.0 to 3.0) % change in the sorption capacity.

3.2.6. Preconcentration and Recovery of the Metal Ions. Enrichment factors for the column method have been determined by increasing the dilution of metal ion solution while keeping the total amount of loaded metal ion fixed at (10 to 20) ng mL^{-1} in the standard and applying the recommended column procedure. The recoveries and enrichment factors achieved at the lowest concentration (lower limit of detection) below which recoveries became nonquantitative are given in Table 8. The data shows that (i) the enrichment factors are very high and ordered as Cu(II) > Co(II) > Ni(II) and (ii) the minimum elution volume of (5, 5, and 6) mL of 2.0 mol L^{-1} HNO_3 is sufficient for the recovery of (99.5, 96.1, and 98.4) % of Cu(II), Ni(II), and Co(II), respectively.

3.2.7. Application the Recommended Method for Determination of Metal Ions in Water Samples. $PsSO_2ASA$ has been used to detect/adsorb preconcentrated Cu(II), Ni(II), and Co(II) in water samples collected from the Arabian Gulf at Kuwait Beach and tap water in Kuwait followed by their determination with ICP-AES. The estimation of the three metal ions has been made without (direct determination) and with standard addition (S.A.) to test its reliability and accuracy by subjecting 2000 mL of the water sample (tap or Gulf) to determine Cu(II) or Co(II) ions and 1500 mL for determination of Ni(II) (in the case of S.A. the samples were spiked with 100 μg of the appropriate metal ion). The data (Table 8) shows the closeness of the direct and S.A., method indicating the reliability of the present method for the metal analysis in water samples.

3.2.8. Comparison with Other Preconcentrating Chelating Resins. The metal capacities and preconcentration factors of $PsSO_2ASA$ have been compared to those of Amberlite XAD-16 supporting resins with different spacers other than the $-SO_2-$ such as Amberlite XAD-16:Gallic acid,[55] Amberlite XAD-16: 2-{[1-(3,4-dihydroxyphenyl)methylidene]amino}benzoic acid,[21] Amberlite XAD-16: 4-{[2-hydroxyphenyl)iminomethyl}-1,2-benzenediol,[56] Anberlite XAD-16: 1,3-dimethyl-3-aminopropan-1-ol[4], Anberlite XAD-16: 1-(2-pyridylazo)2-naphthol[57] and Anberlite XAD-16: calyx[4] resorcinarene[58] and the data are given in Table 10. The data showed that (a) the sorption capacity of Amberlite XAD-16: 4-aminosalicylic acid toward Cu(II) and Co(II) are found to be higher than those of all other chelating resins, while toward Ni(II) is less than the value given for Amberlite XAD-16: 1,3-dimethyl-3-aminopropan-1-ol but higher than the values of all other resins; (b) the preconcentration factor of $PsSO_2ASA$ in case of Cu(II) and Co(II) values are equal to the values of AmberliteXAD-16:Gallic acid and AnberliteXAD-16: 1,3-dimethyl-3-aminopropan-1-ol but more than the preconcentration factors of the others; and (ii) the preconcentration factor of $PsSO_2ASA$ in case of Ni(II) is more than the values found for all resins given in Table 10.

4. CONCLUSION

The novel chelating resin, $PsSO_2ASA$, was synthesized by anchoring 4-aminosalicylic acid to Amberlite XAD-16 through a spacer containing $-SO_2-$ appears promising for the separation of Cu(II), Ni(II), and Co(II) from aqueous media in synthesized and real samples. The chelating resin shows high tendency to form octahedral complexes with these ions through the bonding via the carboxylato and phenolato oxygen atoms. Metal sorption capacities of (601, 473, and 580) μmol g^{-1} and the preconcentration factors of (400, 300 and 333) for Cu(II), Ni(II), and Co(II), respectively, show that $PsSO_2ASA$ is an effective

chelating resin for the separation and preconcentration of the Cu(II), Ni(II), and Co(II) ions in water samples. The resin and the recommended method is also successful in determining metal ions down to the limit of ng mL^{-1}. Furthermore, the data shows that this new chelating resin could be considered very promising and competent as compared to most of the resins reported for determination and preconcentration of the investigated metal ions.

AUTHOR INFORMATION

Corresponding Author
*E-mail: alieldissouky70@yahoo.com.

ACKNOWLEDGMENT

The authors are grateful to Kuwait University for the provision of Grant No. SC 09/06 and the general SAF facility project Grant Nos. GS 01/01 and GS 03/01, and the support of the Faculty of Science, Electron Microscopy Unit is highly appreciated.

REFERENCES

(1) Stephenson, T. *Heavy Metals in Wastewater and Sludge Treatment Processes*; CRC Press: Boca Raton, FL, 1987; Vol. 1 (Sources, Analysis and Legislation).

(2) Kennish, J. M. *Estuarine and Marine Pollution*, CRC Press: Boca Raton, FL, 1997.

(3) Clark, B. R. *Marine pollution*, 5th ed.; Oxford University Press: New York, 2005; Chapters 1, 3, and 5.

(4) Prabhakaran, D.; Subramanian, S. M. A new Chelating Sorbent for Metal Ion Extraction under High Saline Conditions. *Talanta* **2003**, *59*, 1227–1236.

(5) Castillo, M.; Pina-Luis, G.; M.Diaz-Garcia, E.; Rivero, I. A. Solid Phase Organic Synthesis of Sensing Sorbent Materials for Copper and Lead recovery. *J. Braz. Chem. Soc.* **2005**, *16*, 412–417.

(6) Claudia, V. D.; Fiona, M. D.; Martins, H. A. Uptake of Heavy Metals By Chelating Resins From Acidic Manganese Chloride Solution. *Miner. Metallurgical Proc.* **2000**, *17*, 217–222.

(7) Claudia, V. D.; Doyle, M. F.; Ciminelli, T. S. V. Effect of pH on the Adsorption of Selected Heavy Metal Ions From Concentrated Chloride Solutions By the chelating Resin Dowex. *Sep. Sci. Technol.* **2002**, *37*, 3169–3185.

(8) Sun, C.; Ji, R.; Qu, C.; Wang, Q.; Sun, Y.; Cheng, G. A Chelating Resin Containing S, N and O atoms: Synthesis and Adsorption properties of Hg (II). *Eur. Polym. J.* **2006**, *42*, 188–194.

(9) Tanco, L. A. M.; Tanaka, P. A. D.; Flores, C. V.; Nagase, T.; Suzuki, M. T. Preparation of Porous Chelating Resin Containing Linear Polymer Ligand and Adsorption Characteristics for Harmful Ions. *React. Funct. Polym.* **2002**, *53*, 91–101.

(10) Nalwa, H. *Advanced Functional Molecules and Polymers*; Gordan and Breach Science Publishers: Singapore, 2004; Vol. 4.

(11) Perenyi, Z. K.; Lasztity, A.; Hervath, Z.; Levai, A. Use of a New Type of 8-Hydroxyquinoline-5-sulphonic acid cellulose (sulphoxine cellulose) for preconcentration of Trace Metals From Highly Mineralized Water Prior Their GFAAS Determination. *Talanta* **1998**, *47*, 673–679.

(12) Mahmoud, M. E.; Soliman, M. E.; El-Dissouky, A. Metal Uptake Properties of Polystyrene Resin Immobilized Polyamine and Formylsalicylic Acid Derivatives as Chelation Ion Exchangers. *Analyt. Sc. (Jpn.)* **1997**, *13*, 765–769.

(13) Comba, P.; Goll, W.; Nuber, B.; Varnagy, K. Transition Metal Coordination Compounds of Bisamidobispyridyl Ligands. *Eur. J. Inorg. Chem.* **1998**, 2041–2049.

(14) Pramanik, S.; Dhara, S.; Bhattacharyya, S. S.; Chattopadhyay, P. Separation and determination of some metal ions on new chelating resins containing N, N donor sets. *Anal. Chim. Acta* **2006**, *556*, 430–437.

(15) Maurya, R. M.; Kumar, M.; Sikarwar, S. Polymer-anchored oxoperoxo complexes of Vanadium(V),molybdenum(VI) and tungsten-(VI) as catalyst for the oxidation of phenol and styrene using hydrogen peroxide as oxidant. *React. Funct. Polym.* **2006**, *66*, 808–818.

(16) Andrzej, K.; Andrzej, T. W. Novel chelating resins containing calix[4]pyrroles: Synthesis and sorptive properties. *React. Func. Polym.* **2006**, *66*, 740–746.

(17) Kaur, H.; Agraw, Y. K. Functionalization of XAD-4 resin for the separation of Lanthanides using chelation ion exchange liquid chromatography. *React. Funct. Polym.* **2005**, 65277–283.

(18) Saima, M. Q.; Hasany, M. S.; Bhanger, I. M.; Khuhawar, Y. M. Enrichment of Pb(II) ions using phthalic acid functionalized XAD-16 resin as a sorbent. *J. Colloid Interface Sci.* **2005**, *291*, 84–91.

(19) Matsumiya, H.; Yasuno, S.; Iki, N.; Miyano, S. Sulfinylcalix-[4]arene-impregnated Amberlite XAD-7 resin for the separation of niobium(V) from tantalum(V). *J. Chromatogr. A* **2005**, *1090*, 197–200.

(20) Mannar, M. R.; Sweta, S.; Trissa, J.; Halligudi, B. S. Bis(2-[α-hydroxyethyl]benzimidazolato) copper(II) anchored onto chloromethylated polystyrene for the biomimetic oxidative coupling of 2-aminophenol to 2- aminophenoxazine-3-one. *J. Mol. Catal. A: Chem.* **2005**, *36*, 32–138.

(21) Gopalan, V.; Ajai, S. K. 2-{[1-(3, 4-Dihydroxyphenyl)-methylidene]amino}benzoic acid immobilized Amberlite XAD-16 as metal extractant. *Talanta* **2005**, *67*, 187–194.

(22) Kim -Young, S.; Gyo, I.; Han-Cheol, W.; Choi-Jong, M. Studies on synthesis and application of XAD-4-salen chelate resin for separation and determination of trace elements by solid phase extraction. *Microchem. J.* **2005**, *80*, 151–157.

(23) Jeragh, B. J. A.; Elassar., A. A.; El-Dissouky, A. Ligating Behavior and Metal Uptake of N-Sulphonylpolyamine Chelating Resins Anchored on Polystyrene-Divinyl Benzene Beads. *J. Appl. Polym. Sci.* **2005**, *96*, 1839–1846.

(24) Maeve, L. C.; Ana, A.-I.; Robert, F. P.; Kenneth, B. W. Determination of iron and copper in seawater at pH 1.7 with a new commercially available chelating resin, NTA Superflow. *Anal. Chim. Acta* **2005**, *530*, 121–129.

(25) Prabhakaran, D.; Subramanian, S. M. Selective extraction of U (VI) over Th(IV) from acidic streams using Dibis (2-ethylhexyl)malonamide anchored chloromethylated polymeric matrix. *Talanta* **2005**, *65*, 179–184.

(26) Maheswari, A. M.; Subramanian, S. M. XAD-16−3, 4-dihydroxy benzoyl methyl phosphonic acid: a selective preconcentrator for U and Th from acidic waste streams and environmental samples. *React. Funct. Polym.* **2005**, *62*, 105–114.

(27) Sema, C D.; Hayati, F.; Resat, A. Use of an o-aminobenzoic acid-functionalized XAD-4 copolymer resin for the separation and preconcentration of heavy metal(II) ions. *Anal. Chim. Acta* **2004**, *505*, 15–24.

(28) Sibel, Y.; Resat, A. Chromium (III, VI) speciation analysis with preconcentration on a maleic acid- functionalized XAD sorbent. *Anal. Chim. Acta* **2004**, *505*, 25–35.

(29) Yong, G.; Bingjun, D.; Yongwen, L.; Xijun, C.; Shuangming, M.; Maozhong, T. Preconcentration of trace metals with 2-(methylthio)aniline-functionalized XAD-2 and their determination by flame atomic absorption spectrometry. *Anal. Chim. Acta* **2004**, *504*, 319–324.

(30) Schubert, S. U.; Alexeev, A.; Andres, R. P. Terpyridine-Functionalized Tenta Gel Micro beads: Synthesis, Metal Chelation and First Sequential Complexation. *Macromol. Mater. Eng.* **2003**, *288*, 852–860.

(31) Jal, K. P.; Patel, S.; Mishra, K. B. Chemical modification of silica surface by immobilization of functional group for extractive Concentration of Metal Ions. *Talanta* **2004**, *62*, 1005–1028.

(32) Huang, S.-P.; Franz, K. J.; Arnold, E. H.; Devenyi, J.; Fish, D. R. H. Polymer Penant Ligand Chemistry-5. The selective and Competetitive Removal of Ag^{+}, Hg^{2+}, Cu^{2+}, Pb^{2+} and Cd^{2+} ions from Aqueous Solution Utilizing A N- Sulphonylethylenebis-dithiocarbamate) Ligand Anchored on Macroporous Polystyrene-Divinyl benzene Beads. *Polyhedron* **1996**, *15*, 4241–4254.

(33) Tuncel, M.; Özbülbül, A.; Serin, S. Synthesis and characterization of thermally stable Schiff base polymers and their copper(II), cobalt(II) and nickel(II) complexes. *React. Funct. Polym.* **2008**, *68*, 292–306.

(34) Nakamoto, K, *Infrared and Raman Spectra of Inorganic and Coordination Compounds*. 5th ed.; Wiley-Interscience Pub: New York, 1997; pp 153−271.

(35) Nanjundan, S.; Selvamalar, C. S. J.; Jayakumar, R. Synthesis and characterization of poly(3- acetyl- 4-hydroxyphenyl acrylate) and its Cu(II) and Ni(II) complexes. *Eur. Polym. J.* **2004**, *40*, 2313–2321.

(36) Trimukhe, K. D.; Varma, A. J. Metal complexes of crosslinked chitosans: correlations between metal complexation values and thermal properties. *Carbohydr. Polym.* **2009**, *75*, 63–70.

(37) Pehlivan, E.; Altum, T. The study of various parameters affecting the ion exchange of Cu^{2+}, Zn^{2+}, Ni^{2+}, Cd^{2+} and Pb^{2+} from aqueous solution on Doewex 50w synthetic resin. *J. Hazard. Mater.* **2006**, *134*, 149–156.

(38) Lin, H. S.; Lai, L. S.; Leu, G. H. Removal of heavy metals from aqueous solution by chelating resin in a multistage adsorption process. *J. Hazard. Mater.* **2006**, *76*, 139–153.

(39) Leinonen, H.; Lehto, J. Ion exchange of nickel by iminodiacetic acid chelating resin chelx 100. *React. Funct. Polym.* **2000**, *43*, 1–6.

(40) Chen, Y. C. Stability constants of water soluble and latex types of chelating Polymers containing iminodiacetic acid with some transition metal ions. *Eur. Polym. J.* **2003**, *39*, 991–1000.

(41) Lagergren, S.;*Zur theorie der sogenannten adsorption geloster-stoffe*; Kungliga Svenska Vetenskapsakademiens: Handlingar, 1898; Vol. *24*, pp 139.

(42) Ho, S. Y.; McKay, G. Pseudo-second order model for sorption processes. *Process Biochem.* **1999**, *34*, 451–465.

(43) Guibal, E.; Milot, C.; Tobin, M. J. Metal-anion sorption by chitosan beats: equilibrium and kinetic studies. *Ind. Eng. Chem. Res.* **1998**, *37*, 1454–1463.

(44) Cheung, W.; Ng, Y.; Mckey, G. Kinetic analysis of the sorption of copper (II) ions on chitosan. *J. Chem. Technol. Biotechnol.* **2003**, *78*, 562–571.

(45) Ho, S. Y.; Mckay, G. The kinetics of sorption of divalent metal ions onto Sphagnum Moss Peat. *Water Res.* **2000**, *34*, 735–742.

(46) Yurdakoç, M.; Scki, Y.; Yuedakoç, K. S. Kinetic and thermodynamic studies of boron removal by siral 5, Siral 40 and Siral 80. *J. Colloid Interface Sci.* **2005**, *286*, 440–446.

(47) Wu, F. C.; seng, R. L.; Juang, R. S. Kinetic modeling of liquid-phase adsorption of reactive dyes and metal ions on chitosan. *Water Res.* **2001**, *35*, 613–618.

(48) Wu, C.-H. Adsorption of reactive dye onto carbon nanotubes: Equilibrium, kinetics and thermodynamics. *J. Hazard. Mater.* **2007**, *144*, 93–100.

(49) Zhou, L.; Wang, Y.; Liu, Z.; Huang, Q. characteristics of equilibrium, kinetic studies for adsorption of Hg(II), Cu(II) and Ni(II) ions by thiourea-modified magnetic chitosan microspheres. *J. Hazard. Mater.* **2009**, *161*, 995–1002.

(50) Qi, X.; Jia, X.; Yang, Y. Niu, Li-e. Formation and recovery of Co^{2+}, Ni^{2+}, Cu^{2+} macromolecular complexes with polystyrene and acrylic acid. *Hydrometer* **2009**, *96*, 269–274.

(51) Jing, X.; Liu, F.; Yang, X.; Ling, P.; Li, L.; Long, C.; Li, A. Adsorption performances and mechanisms of the newly synthesized N, N′-di(carboxymethyl)dithiocarbamate chelating resin toward divalent heavy metal ions from aqueous media. *J. Hazard. Mater.* **2009**, *167*, 589–596.

(52) Langmuir, I. The concentration and fundamental properties of solids and liquids. *J. Am. Chem. Soc.* **1916**, *38*, 2221–2295.

(53) F.M.H. Freundlich, I. Over the adsorption in solution. *Z. Phys. Chem.* **1906**, *57*, 385–470.

(54) Qi, L.; Xu, Z. Lead sorption from aqueous solutions on chitosan nanoparticales. *J. Colloid Interface Sci.* **2004**, *251*, 186–193.

(55) Sharma, R. K.; Pant, P. Preconcentration and determination of trace metal ions from aqueous samples by newly developed gallic acid modified Amberlite XAD-16 chelating resin. *J. Hazard. Mater.* **2009**, *163*, 295–301.

(56) Venkatesh, G.; Singh, A. K. 4-{[2-hydroxyphenyl)imino-methyl}-1,2-benzenediol (HIMB) anchored Amberlite XAD-16: Preparation and applications as metal extracts. *Talanta* **2007**, *71*, 282–287.

(57) Narin, I.; Soylak, M.; Kayakirilmaz, K.; Elci, L.; Dogan, M. Preparation of a chelating resin by immobilizing 1-(2-pyridylazo)-2-naphthol on Amberlite XAD-16 and its application of solid phase and Extraction of Ni(II), Cd(II), Co(II), Cu(II), Pb(II) and Cr(III) in natural water samples. *Anal. Lett.* **2003**, *36*, 641–658.

(58) Ghaedi, M.; Karami, B.; Ehsani, Sh.; Marahel, F.; Soylak, M. Preconcentration-separation of Co^{2+}, Ni^{2+}, Cu^{2+} and Cd^{2+} in real samples by solid phase extraction of a calyx[4] resorcinarene modified Amberlite XAD-16 resin. *J. Hazard. Mater.* **2009**, *172*, 802–808.